

Springtime Fire Weather in Tasmania, Australia: Two Case Studies

PAUL FOX-HUGHES

*Bureau of Meteorology, and Institute for Marine and Antarctic Studies, University of Tasmania,
Hobart, Tasmania, and Bushfire Cooperative Research Centre, East Melbourne, Victoria, Australia*

(Manuscript received 13 February 2011, in final form 20 November 2011)

ABSTRACT

A number of severe springtime fire weather events have occurred in Tasmania, Australia, in recent years. Two such events are examined here in some detail, in an attempt to understand the mechanisms involved in the events. Both events exhibit strong winds and very low surface dewpoint temperatures. Associated 850-hPa wind–dewpoint depression conditions are extreme in both cases, and evaluation of these quantities against a scale of past occurrences may provide a useful early indicator of future severe events. Both events also feature the advection of air from drought-affected continental Australia ahead of cold fronts. This air reaches the surface in the lee of Tasmanian topography by the action of the föehn effect. In one event, there is good evidence of an intrusion of stratospheric, high potential vorticity (PV), air, supplementing the above mechanism and causing an additional peak in airmass dryness and wind speed.

1. Introduction

Tasmania, located south of the Australian continent (Fig. 1), shares with other parts of southeastern Australia a history of frequent fire weather and fire events, including occasional fire disasters (Bond et al. 1967; Bureau of Meteorology 1985; Mills 2005a,b; Nairn et al. 2005). “Fire weather” refers to weather events resulting in higher than average temperatures, low relative humidity, and strong wind, often following periods of low rainfall when vegetation will be particularly combustible.

Episodes of low humidity and strong wind are a normal springtime feature of the Australian subtropics (Luke and McArthur 1978, p. 15), parts of North America (Westerling et al. 2006), and of the Eurasian boreal forests (e.g., Stocks and Lynham 1996; Valendik et al. 1998). Such regimes can have a significant impact on fire, marine, agricultural, aviation, and public weather users. On the other hand, the season of peak fire weather in Tasmania has commonly been regarded as late summer into autumn (Luke and McArthur 1978, p. 15). Among fire managers and meteorologists, however, there has been discussion of a springtime “bump,” or early season peak in fire danger, subsiding before the primary seasonal

peak occurred some months later. This springtime bump has been documented (Fox-Hughes 2008) as occurring in October or November, roughly one year in two.

Over much of Australia, fire danger in forested areas is estimated using the McArthur Forest Fire Danger meter Mark V (McArthur 1967). The resulting forest fire danger index (FFDI) is a function of temperature, relative humidity, (10-min average), wind speed, and fuel moisture; the latter encoded as a “drought factor” representing the substantial forest fuel availability. Fox-Hughes (2008) examined FFDI values computed from synoptic observations at several Tasmanian sites, establishing that the springtime secondary peak is a feature of the east and southeast of the state.

Springtime fire weather is of concern for several reasons. Scientifically, it is of interest to know whether its recent increase in frequency is a response to a secular trend, or part of a long-term climatic cycle. Understanding the synoptic environments in which dangerous springtime fire weather occurs opens the possibility of linking such events to broader-scale drivers, and seasonal prediction of “bad” springtimes. Operationally, it is important for fire managers to be aware of the potential for the occurrence of such events and to prepare accordingly, during periods when resources are often still being allocated and when planning is being undertaken for the fire season peak. Fire weather forecasters are therefore also particularly sensitive to the occurrence

Corresponding author address: Paul Fox-Hughes, Bureau of Meteorology, 111 Macquaries St., Hobart TAS 7000, Australia.
E-mail: p.fox-hughes@bom.gov.au

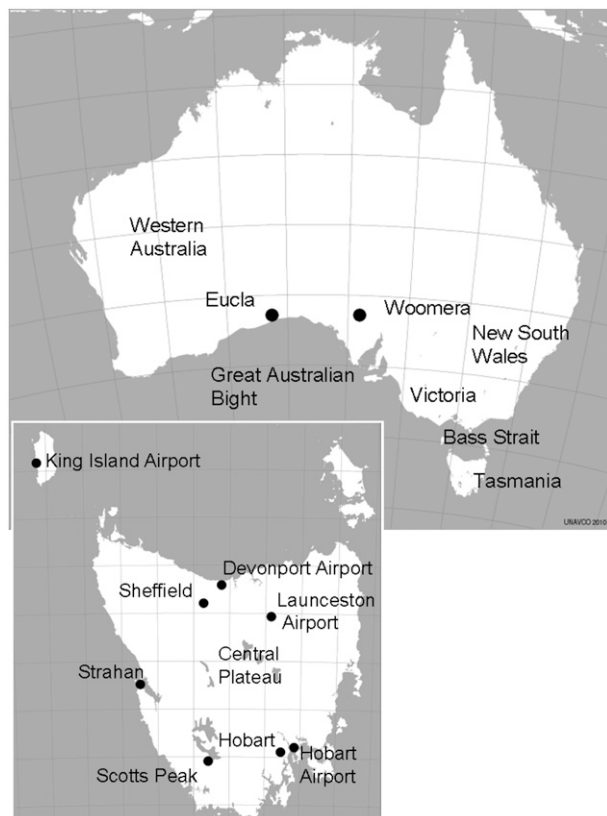


FIG. 1. Location of Tasmania and other places mentioned in this paper.

of these events, and need to be alert during the early fire weather season to indicators that a springtime fire weather event may develop. As part of a research effort to understand the nature and influences on the springtime peak, this study examines two events in some detail. The study forms a step between an observational station-based analysis establishing the existence of the springtime fire danger peak (Fox-Hughes 2008) and future studies aimed at improving the predictability of both individual springtime fire weather events and, more broadly, seasons during which such events are more likely to occur. In the following sections, the selection of events for investigation will be discussed, and each event will be presented in its synoptic and mesoscale setting. Common characteristics will be examined and differences explored.

2. Events and data

Both events examined here were very significant fire weather occurrences, characterized particularly by periods of surface dry air exceptional in the Tasmanian climate record. Thus, the immediate origin of the surface dry air pulses will be a focus of event descriptions.

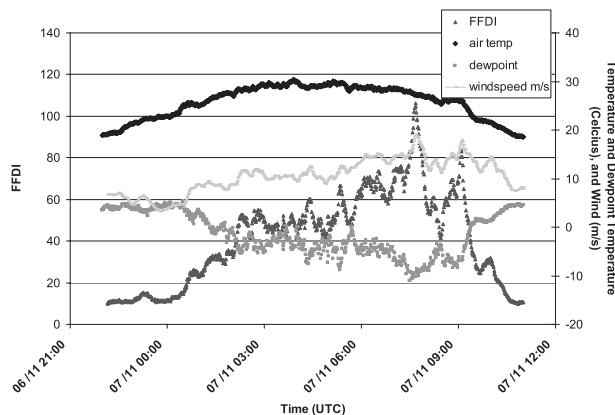


FIG. 2. Plot of air temperature ($^{\circ}\text{C}$, thick black), dewpoint temperature ($^{\circ}\text{C}$, thick gray), wind speed (km h^{-1} , thin dark gray), and FFDI (black triangles) at the Hobart airport on 7 Nov 2002.

On 7 November 2002, a late afternoon–early evening cool change was preceded by strong to gale force winds, with very warm, dry air. Approximately 40 wildfires were ignited in eastern Tasmania (Bureau of Meteorology 2002, p. 2). The fire danger was “very high” ($\text{FFDI} > 24$) from early afternoon through midevening, peaking during the early evening as wind speeds increased and dewpoint temperatures fell immediately ahead of the front.

The week prior to 12 October 2006 was characterized by persistent very dry air over Tasmania. Successive frontal passages caused fire danger episodes on preceding days, and gale-strength prefrontal winds on 12 October resulted in exceptional fire weather. A 800-ha fire on the outskirts of Tasmanian state capital city, Hobart, nearly destroyed many dwellings. In the event, a remarkable combination of preparedness and wind direction prevented significant structural damage.

Both cases are examined using archived data from the Australian Bureau of Meteorology’s mesoscale version of the Limited Area Prediction System (LAPS) model (mesoLAPS; Puri et al. 1998). In 2002, the grid resolution of mesoLAPS was 12.5 km. By October 2006, a number of subdomains existed with 5-km resolution, including one encompassing Tasmania.

3. 7 November 2002

a. Surface weather and forest fire danger on 7 November 2002

Weather parameters and FFDI from the Hobart airport on 7 November are plotted in Fig. 2. Data points are instantaneous values of temperature and dewpoint every minute, with 10-min-averaged wind speed, again available every minute. The drought factor throughout the day remained at 9 (indicating 90% of fine fuel

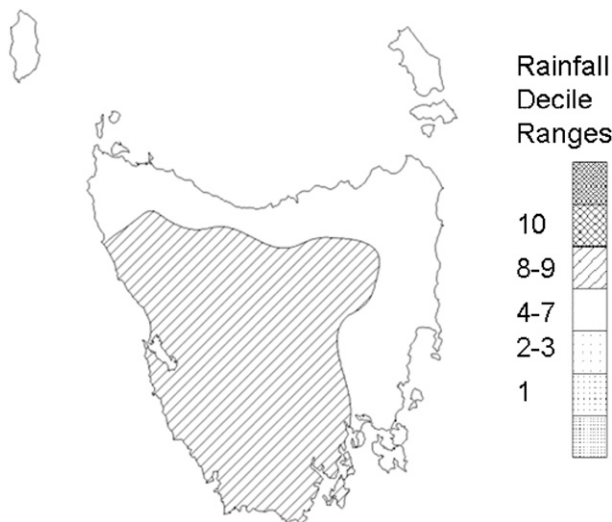


FIG. 3. Tasmanian rainfall deciles for the 3-month period 1 Aug–31 Oct 2002. Shading indicates that much of Tasmania experienced above average (decile 8–9) late winter to early spring rainfall while the eastern and northern coastal fringes were close to average (decile 4–7). The image was generated with gridded data from the National Climate Center of the Australian Bureau of Meteorology.

available to burn). FFDI increased rapidly soon after midday (0100 UTC) as dewpoint fell to around -5°C and wind increased to $30\text{--}40\text{ km h}^{-1}$, mostly exceeding 50 km h^{-1} between 0530 and 0900 UTC. FFDI peaked over 100 at 0740 UTC as the dewpoint temperature fell to -11°C and the wind speed increased above 60 km h^{-1} . A secondary peak occurred at 0900 UTC, as the dewpoint temperature briefly dropped again to -8°C . Subsequently, FFDI fell as the wind speed and temperature decreased while the dewpoint temperature rose. The event was unusual because of the magnitude of the peak FFDI and because it occurred later than any other FFDI peak greater than 50 recorded at the Hobart airport.

b. Antecedent conditions

Conditions prior to 7 November 2002 had been unexceptional. Tasmanian rainfall for October 2002 was close to average and, for the 3 months of August–October, average in the east, and largely above average in western and central areas (Fig. 3). Consequently, fuel moisture levels were typical of midspring. It is worth noting, however, that much of Australia had experienced below or very much below average rainfall during August–October 2002. Persistent very dry conditions in Australia led to a prolonged period of bushfires in New South Wales in late 2002 (Taylor and Webb 2004), and to devastating fires in Canberra (McLeod 2003; Mills 2005b) and in alpine regions of Victoria in early 2003 (Bureau of Meteorology 2003).

c. MSLP progression

During early November 2002, several fronts crossed Tasmania as a high pressure system slowly moved eastward across the Great Australian Bight (Fig. 4a). By 0000 UTC 6 November (Fig. 4b), the high had moved over southeastern Australia, east of the bight, and ridged southward over western Tasmania. Another front was progressing steadily eastward within a broad trough south of Western Australia, with a prefrontal trough developing by 1800 UTC 6 November (Fig. 4c), a common feature of Australian warm season frontal systems (Hanstrum et al. 1990). Frontogenesis occurred in the cold air behind the front as it moved east, and a low pressure system developed rapidly during 7 November in the trough in which the trailing front itself had formed (Fig. 4d). The fronts crossed Tasmania during the early evening of 7 November, as the low pressure system moved to the east near 50°S .

d. Upper-level and satellite analysis

Figures 5a and 5b display mesoLAPS forecast winds initialized at 1200 UTC 6 November at 300 hPa around Tasmania. The upper-level trough associated with the approaching frontal system can be seen in Fig. 5a at 1800 UTC 6 November near 125°E . A broad jet stream lobe ahead of the trough is evident over waters west and south of Tasmania, while that to the rear of the trough is just visible on the far left of the figure.

Over the 12 h to 0600 UTC 7 November (Fig. 5b), the trough axis advanced to just east of 135°E , and the trough became slightly negatively tilted, with the left entrance region of the leading jet streak immediately southwest of Tasmania. Subsequently (not shown), the 50 m s^{-1} isotach extended through the apex of the trough at 0900 UTC, linking the jet streaks flanking the trough. The trough itself passed immediately south of Tasmania around 1200 UTC.

Rapid development of the secondary front and low to the south during 7 November is evident on in *Geostationary Operational Environmental Satellite-9* (GOES-9) infrared imagery at 2030 UTC 6 November and 0530 UTC 7 November (Figs. 6a and 6b, respectively). Frontal cloud is poorly organized at 2030 UTC west of Tasmania between 130° and 140°E , with cloud corresponding to the prefrontal trough near the head of the bight, around 35°S , 125°E . The frontogenetic region west of the primary front is evident as a solid band of NW–SE-oriented mid- to high-level cloud extending back from near 50°S , 123°E . Over eastern Tasmania, a region of “banner” cloud had formed, moving offshore during the day as the fronts approached and allowing several hours of sunny conditions to enhance mixing of boundary layer air with higher-momentum, drier air above.

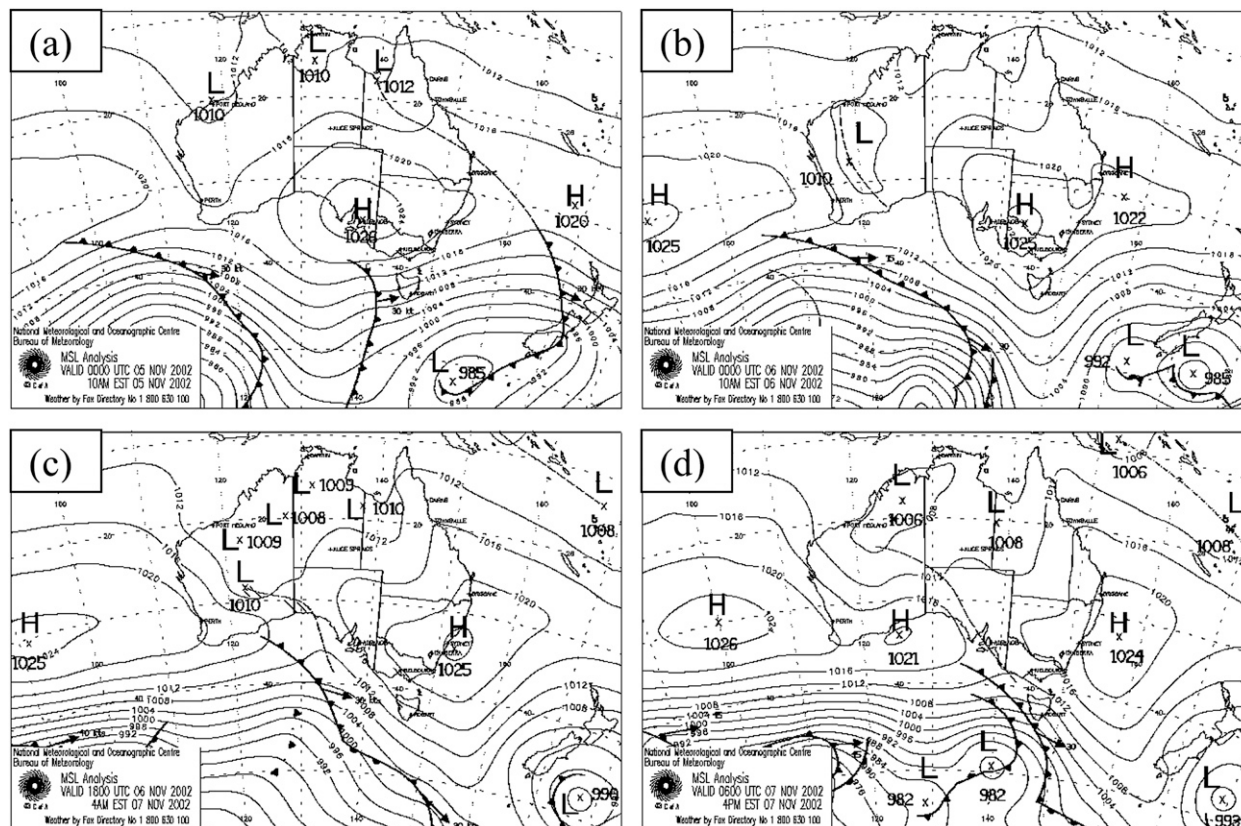


FIG. 4. MSLP Australian region charts at (a) 0000 UTC 5 Nov, (b) 0000 UTC 6 Nov, (c) 1800 UTC 6 Nov, and (d) 0600 UTC 7 Nov 2002.

By 0530 UTC, the fronts had moved rapidly toward Tasmania. The 0530 UTC IR image indicates an area of generally clearer sky over much of eastern Tasmania than had been the case earlier, with an area of cloud immediately east of Tasmania, likely banner cloud displaced somewhat eastward of its earlier position. In

the west, however, incursion of mid- to high-level cloud associated with the approaching fronts had commenced. Their surface position was likely just off the west coast at the time. The second front displays a classic mid- to upper conveyor belt above the surface feature, suggesting that it had matured rapidly during the day.

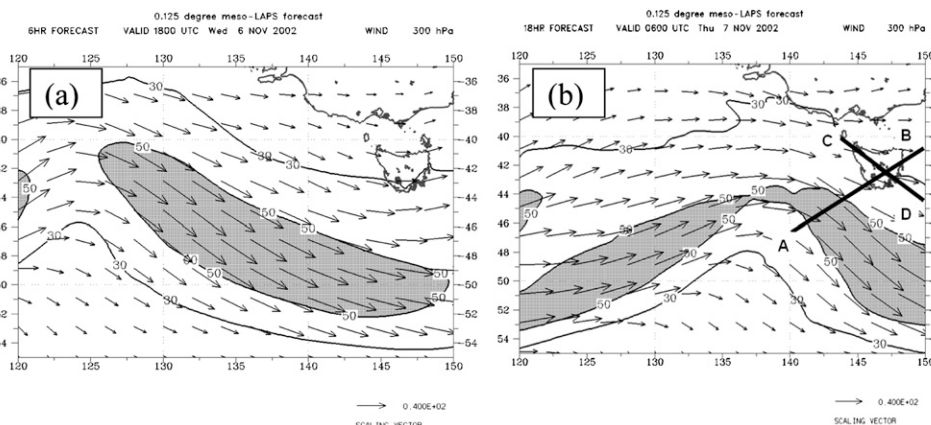


FIG. 5. Charts of 300-hPa wind over and west of Tasmania, from the mesoLaps forecast initialized at 1200 UTC 6 Nov 2002, at (a) 1800 UTC 6 Nov (6-h forecast) and (b) 0600 UTC 7 Nov 2002 (18-h forecast). Wind speed is in m s^{-1} with areas $>50 \text{ m s}^{-1}$ indicated in gray. Solid lines in (b) identify model cross sections in Figs. 10 and 12.

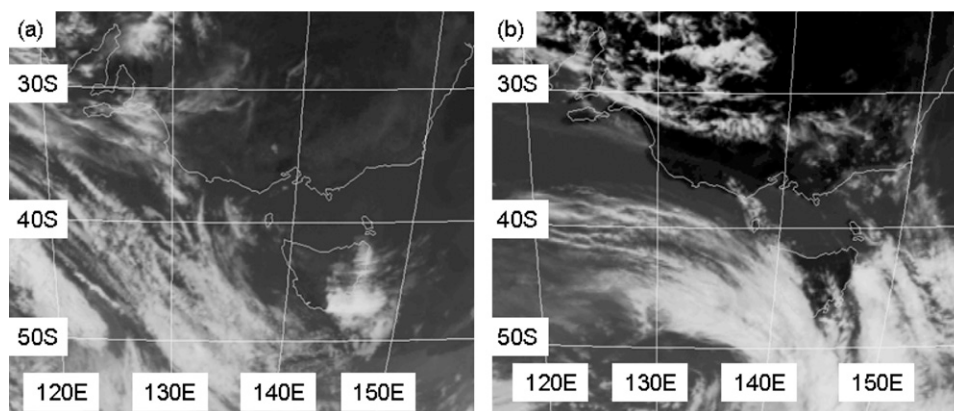


FIG. 6. The IR satellite images over southeastern Australia at (a) 2030 UTC 6 Nov and (b) 0530 UTC 7 Nov, from *GOES-9*.

It is likely that the driest, high-momentum air was associated with the passage across Tasmania of a “dry band” (Mills 2008) in the water vapor imagery. The 0426 UTC *GOES* WV image (Fig. 7) shows the main frontal cloud band clearly visible as an area of white, and the clear space over Tasmania evident from the IR images is revealed as a significant, though narrow, dry band extending back across western Victoria to a broad region of very dry air aloft over the Great Australian Bight. While the area of dry air over the bight existed in previous images (not shown), the filament that crossed Tasmania during the afternoon only became visible during the day, as the frontal cloud band became more organized.

e. Airmass characteristics

Figure 8a shows the routine Hobart airport radiosonde flight at 2300 UTC 6 November. The dewpoint temperature at 850 hPa was -18°C , in the lowest 5% of 850-hPa dewpoint temperature measurements since 1992. Further, the driest air in the troposphere occurred in a layer between about 930 and 740 hPa. Once the surface temperature reached $29^{\circ}\text{--}30^{\circ}\text{C}$, the lapse rate would have been close to dry adiabatic from the surface through this layer to almost 600 hPa. Indeed, as the temperature rose to 29°C , the dewpoint temperature fell to -4° to -5°C . The airport sounding at Hobart suggests that the mean mixing ratio through the lowest third (or more) of the troposphere was about 2.6 g kg^{-1} , corresponding to a dewpoint temperature of -5°C at the surface. It is clear, then, that mixing had occurred through the lower several hundred hectopascals of the atmosphere by early afternoon.

Back trajectories for 120 h ending 0000 UTC 7 November immediately around Hobart are shown in Fig. 9, for parcels ending at a height of 1500 m above ground level. The back trajectories were calculated from mesoLAPS NWP model output, using the National Oceanic and Atmospheric Administration’s (NOAA)

Hybrid Single Particle Lagrangian Integrated Trajectory Model (HYSPLIT; Draxler and Hess 1998). Trajectories were computed for 16 points on a square centered on Hobart, separated by 0.05° , approximately 5 km at the latitude of Hobart, allowing assessment of any divergence in the air parcel paths. As indicated in Fig. 9, the 16 air parcels follow very similar trajectories out to 72 h, increasing confidence that they represent the path followed by the air mass experienced at Hobart during the late morning. Between 0000 UTC on 2 November and 0000 UTC on 4 November, most parcels experienced sustained descent from above 5000 m over waters south of the Australian continent. (Corresponding back trajectories for 0300 UTC 7 November, not shown, reveal that all parcels originated high in the troposphere southwest of Australia.) By 0000 UTC on 4 November, the air parcels were located inland of the head of the Great

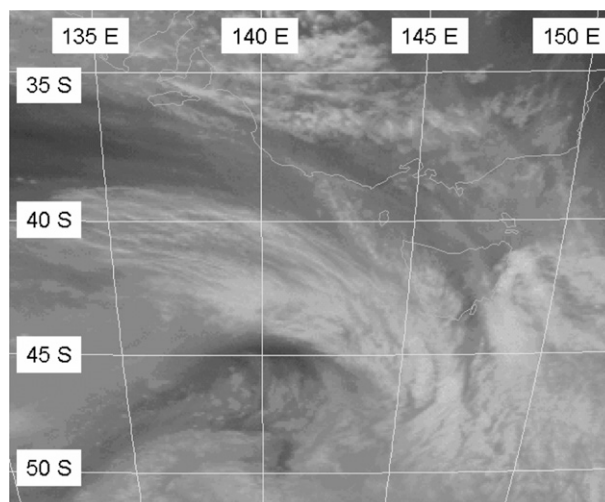


FIG. 7. *GOES* WV image at 0426 UTC 7 Nov over southeastern Australia. White areas indicate high cloud while dark areas indicate mid- to high-level dry air.

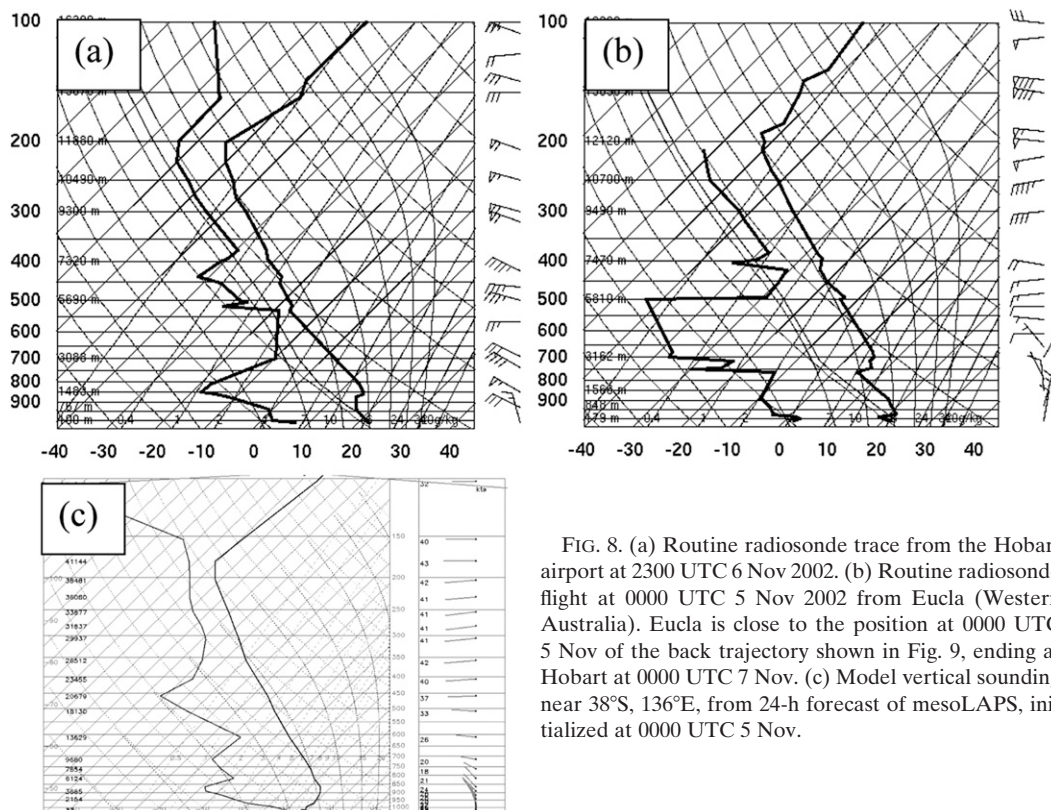


FIG. 8. (a) Routine radiosonde trace from the Hobart airport at 2300 UTC 6 Nov 2002. (b) Routine radiosonde flight at 0000 UTC 5 Nov 2002 from Eucla (Western Australia). Eucla is close to the position at 0000 UTC 5 Nov of the back trajectory shown in Fig. 9, ending at Hobart at 0000 UTC 7 Nov. (c) Model vertical sounding near 38°S, 136°E, from 24-h forecast of mesoLAPS, initialized at 0000 UTC 5 Nov.

Australian Bight, at an elevation of around 2000 m. At that time, this position was close to the center of the high that subsequently moved eastward. The elevation profile for the back trajectories indicates that air parcels subsided through the high, moving southward and into its western flank by 0000 UTC 5 November, before being entrained into the prefrontal northwesterly flow at an elevation of around 1500 m. During 6 November, parcels sank farther to about 1000 m before beginning to rise, consistent with their poleward trajectory and ultimately in response to encountering Tasmanian orography, before sinking abruptly in the lee of the western Tasmanian range over Hobart. At 0000 UTC 5 November, the model parcels were near the upper-air station in Eucla, Western Australia. The Eucla sounding at that time (Fig. 8b) shows a dry air mass between 1000- and 2500-m elevation, with a dewpoint temperature near -10°C , quite consistent with the air over Hobart 48 h later. Modeled back trajectories of parcels ending at 1500 m above Hobart later in the day (not shown) indicate a broadly similar path. It is likely, then, that the 2300 UTC sounding is representative of the air mass over Hobart for much of the day.

The air mass over Hobart on 7 November experienced a long overwater trajectory, raising the possibility that

its moisture content increased while it traversed the Great Australian Bight (and that the dry air observed was not of continental origin). A 24-h forecast model vertical sounding from the mesoLAPS operational run at 0000 UTC 5 November is displayed in Fig. 8c, revealing the presence of a marine boundary layer below an inversion at about 900 hPa. There is a steep decline with height in dewpoint temperature within the boundary layer, and largely dry, continental, air above. The stability of the inversion layer likely prevented mixing between the two layers, with minimal transport of moisture into the overlying air mass.

f. Mesoscale features

Cross sections from mesoLAPS run at 1200 UTC 6 November, along the line AB in Fig. 5b, are displayed in Fig. 10, valid at 0600 UTC on 7 November. The left-hand extremity in Fig. 10 corresponds to the location of the center of the trough at that time. The tropopause height is depressed, as indicated by the cluster of potential vorticity unit (PVU; where $1 \text{ PVU} = 10^{-6} \text{ m}^2 \text{ s}^{-1} \text{ K kg}^{-1}$) isopleths dropping from approximately 250 hPa over Tasmania to near 450 hPa, close to the trough axis. A region of relative humidity below 30% extends from immediately under this level to 700 hPa in the direction of

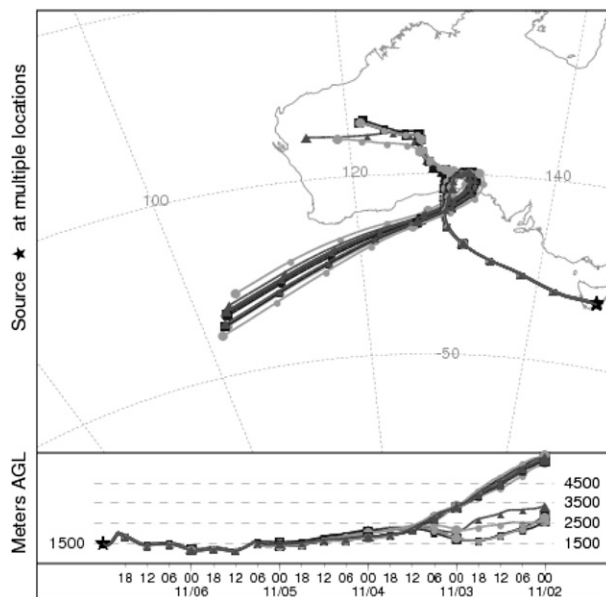


FIG. 9. Modeled back trajectories of air parcels ending at 1500 m above ground level over Hobart at 0000 UTC 7 Nov. (top) Plan view of parcel movement over a 120-h period. (bottom) A cross section (height in m) of the parcel trajectories. In both cases, a high degree of conformity is evident in the path taken by parcels to reach the cluster of endpoints around Hobart.

Tasmania, approximately along the 300-K potential temperature isopleth (Fig. 10b). Also evident in Fig. 10a and extending along this axis is a well-defined region of anomalous PV, indicating a PV intrusion from the tropopause depression farther west. In the center of Fig. 10a, above about 600 hPa, an area of high relative humidity is evident, corresponding to the frontal cloud band that can be seen in Figs. 6 and 7. Figure 11 is a pseudo-water vapor (WV) image generated from mesoLAPS for 0600 UTC 7 November, close to the time of the GOES WV image in Fig. 7, presenting a different perspective on the mesoLAPS information. The frontal cloud band is clearly visible, as is the dry area immediately to its west and south associated with upper-level descent. The pseudo-WV image provides a method of quickly assessing whether the model has resolved essential features of the atmospheric development, by comparison with actual WV imagery (see, e.g., Georgiev and Martin 2001). In this case, the correspondence between the two images of the frontal band, the tropopause descent near the trough axis and broad descent over the Great Australian Bight, suggest that key aspects of the dynamics have been captured by mesoLAPS.

Figure 10b plots isentropes and isotachs along cross-section AB. The model atmosphere appears well mixed to 850 hPa near Hobart, but substantially less so over the water on either side of the Tasmanian landmass. The

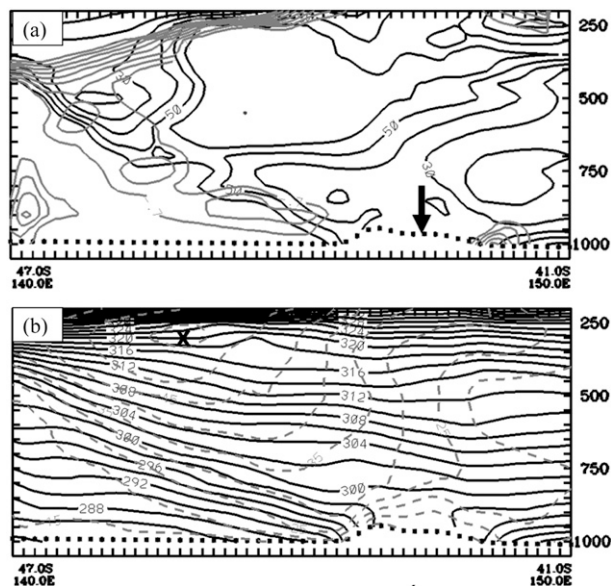


FIG. 10. Cross sections through the line AB in Fig. 5b at 0600 UTC 7 Nov, from the 18-h forecast of mesoLAPS initialized at 1200 UTC 6 Nov, showing (a) RH (black), at intervals of 10%, between 10% and 60%, and potential vorticity (gray), at intervals of 0.2 PVU between -0.7 and -2.1 PVU. The approximate location of Hobart is indicated by an arrow. (b) Potential temperature isentropes (black) at intervals of 2 K, and wind speed (gray, dashed) isotachs at intervals of 5 m s^{-1} . Location of the jet core is indicated by an X.

jet maximum of 50 m s^{-1} near 250 hPa is immediately below the tropopause. A lobe of increased wind speed descends from the jet toward Tasmania along the same axis as the relative humidity minimum. Within this lobe,

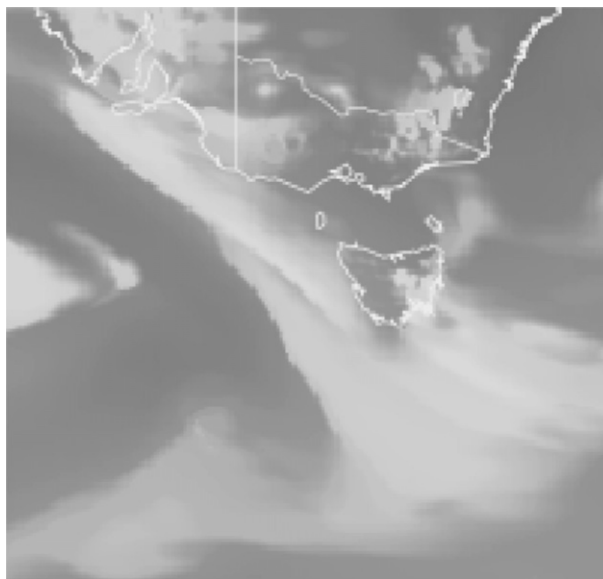


FIG. 11. Pseudo-WV image generated from mesoLAPS initialized at 1200 UTC 6 Nov, valid 0600 UTC 7 Nov.

the 30 m s^{-1} contour descends to 900 hPa, clearly within the boundary layer during the afternoon, suggesting the possibility of gusts at the surface to around that value. The slantwise descent of this dry, high-momentum air in the frontal zone places it over southeast Tasmania within the upper part of the boundary layer, as judged from the Hobart sounding earlier in the day, allowing it then to mix to the surface to cause the observed evening FFDI peak.

Further, the 2300 UTC 6 November sounding from the Hobart airport shows that the top of the boundary layer during the afternoon of 7 November was at about 3000 m. Back trajectories to 120 h ending at 3000 m above Hobart (not shown) at 0000 and 0600 UTC show an airmass origin over the waters south of Western Australia at a height of about 3000 m at 0000 UTC, rising to about 4000 m by 0600 UTC. Thus, the air at the top of the boundary layer, capable of mixing to the surface by late afternoon, came from higher in the atmosphere during the afternoon than was the case during the morning. This can account for the increase in FFDI late in the day: the higher-level air was drier and carried greater momentum than that lower in the atmospheric column.

The air mass over Hobart during much of the afternoon of 7 November was of northwesterly origin. Back trajectories of air parcels immediately above the surface at 0600 UTC 7 November (not shown) indicated that, during the morning, parcels had been immediately west of Bass Strait, on a trajectory along the line CD in Fig. 5b. Vertical cross sections of the model atmosphere along this line are shown in Fig. 12. With respect to the northwesterly flow direction, Hobart lies in the lee of the central Tasmanian orography, much of which is over 1000 m above sea level. In Fig. 12a, over much of the land area a well-mixed lower atmosphere can be seen aloft, as discussed earlier. On the windward side of the island, however, there is strong evidence for a marine boundary layer in the lowest few hundred meters, with a rapid decrease in potential temperature up to the 300-K isentrope. In Fig. 12b, vertical motion along CD is shown, with contours every 20 hPa h^{-1} (negative values dashed). Upward motion in excess of 85 hPa h^{-1} is evident above the windward coast, while in the immediate lee of the highest orography air descending at more than 75 hPa h^{-1} can be seen. Weaker descent (15 hPa h^{-1} or more) occurs over Hobart. This pattern of features is characteristic of a föehn effect, which would have contributed to warming and drying of the air over Hobart during 7 November. The mountain wave aspect of the föehn effect would also have contributed to the descent of the anomalous PV air identified above. Sharples et al. (2010) discuss föehn winds within a context of southeast Australian fire weather, highlighting very similar structures of vertical motion over orography in other fire weather events. They also discuss

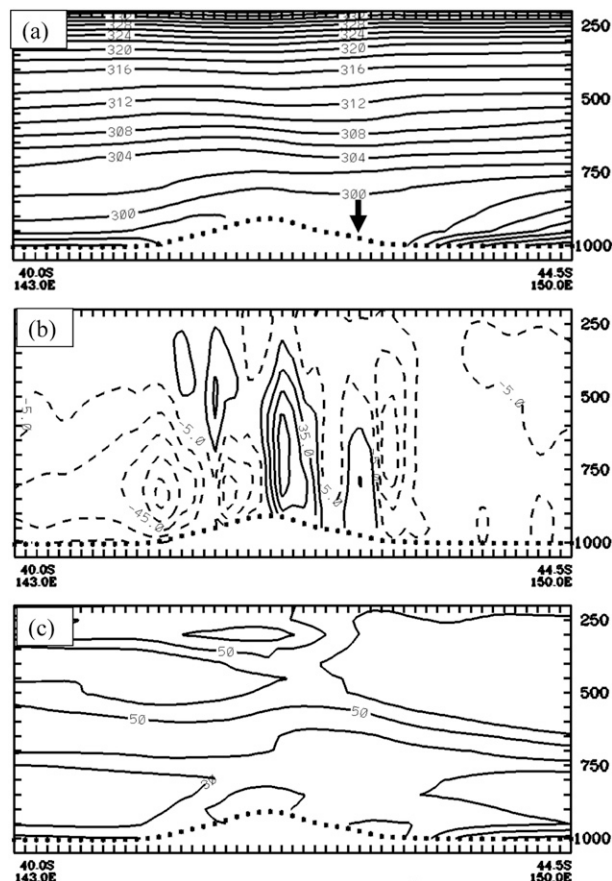


FIG. 12. MesoLAPS forecast cross sections through the line CD in Fig. 5b, initialized at 1200 UTC 6 Nov, valid 0600 UTC 7 Nov. The cross sections show (a) potential temperature (K, interval = 2 K), with the approximate location of Hobart indicated by an arrow; (b) vertical motion [hPa h^{-1} , contoured every 20 hPa h^{-1} , with negative (upward) values dashed]; and (c) RH, contoured every 10% between 10% and 60%.

the importance of orographic blocking of moist low-level air upstream from the area subject to föehn winds, evidenced in Fig. 12a.

The alignment of upper- and lower-atmospheric processes sometimes occurs to allow advection of very dry air from near-stratospheric levels to the surface. Huang et al. (2009) diagnose the descent of upper-tropospheric, exceptionally dry, air to the planetary boundary layer through the mechanism of the transverse ageostrophic circulation in the exit region of a jet streak moving southward over the western United States. Coupled with lower-atmospheric conditions conducive to the development of severe downslope winds in the lee of southern Californian ranges, the dry air was conveyed to the surface to produce dangerous fire weather conditions. Zimet et al. (2007) described a similar occurrence contributing to dangerous fire weather conditions at Mack Lake, in the Great Lakes region of North America. Charney and Keyser (2010) discuss the

meteorological conditions contributing to the spread of a wildfire in the Double Trouble State Park in New Jersey. Again, downward transport of dry, high-momentum mid-tropospheric air into a deep mixed boundary layer caused a rapid increase in fire danger during the day. Mills (2008) investigates the association of WV dry bands with surface drying in Australia, hypothesizing the descent of upper-tropospheric air to the top of the boundary layer via dynamic processes, and its further descent to the surface through deep boundary layer mixing. It is very likely that the same processes operated on and prior to 7 November 2002, in which a small-scale feature developed over the course of several days and became evident in the satellite WV imagery and clear from its impact on surface weather parameters in southeast Tasmania, advected air from high levels to heights at which thermal and mechanical mixing could ensure the descent of that air to the surface.

4. 12 October 2006

a. Surface weather and forest fire danger: 11–12 October

FFDI values recorded on Thursday, 12 October, were comparable to those measured on 7 February 1967. On that date, FFDI peaked at 128, the highest calculated in a dataset of 3-hourly synoptic observations from 1960 to 2006. Devastating bushfires occurred in southeastern Tasmania, killing 62 people and destroying more than 1400 major buildings. Bond et al. (1967) describe this event, while Fox-Hughes (2008) places it in a climatological context. On 12 October, FFDI calculated from the same set of synoptic observations peaked at 126 at the Hobart airport. FFDI calculated from data recorded every minute, as described in connection with the case of 7 November 2002, resulted in a peak FFDI of 133 (Fig. 13). The FFDI at the Hobart airport remained above 100 for at least 90 min in the late morning and, again, during the afternoon. (It is worth noting that the peak FFDI on 7 February 1967 occurred over a single period of about an hour.) Further, four locations in southeast Tasmania reported FFDI of 100 or more during 12 October.

Individual weather parameters used to calculate FFDI were similarly extreme, as might be expected. The maximum temperature recorded at Hobart on 12 October was 33.1°C, the third-highest October maximum recorded at the site, and the warmest since a record of 34.6°C was set on 31 October 1987. A number of sites recorded wind gusts in excess of 100 km h⁻¹, and Hobart recorded a gust to 93 km h⁻¹. The 10-min mean wind at the Hobart airport during the period 0000–0800 UTC was generally between 50 and 60 km h⁻¹. Through much of southeast Tasmania relative humidity fell below 10% on both 11

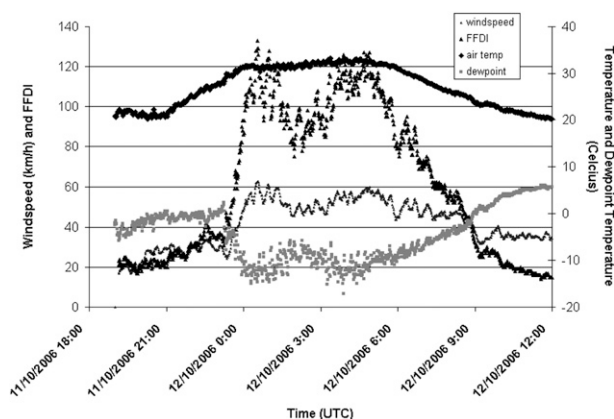


FIG. 13. Plot of air temperature (°C, thick black), dewpoint temperature (°C, thick gray), wind speed (km h⁻¹, thin dark gray), and FFDI (black triangles) at the Hobart airport on 12 Oct 2006.

and 12 October, and was as low as 4% during the afternoon of 12 October at the Hobart airport.

The final, very significant, feature of the event was its longevity. It has already been noted that the Hobart airport experienced an extended period of FFDI greater than 100. FFDI at a Hobart city observation site, 15 km to the west, was “very high” from 2239 UTC on 10 October until 0915 UTC the following day, when a cool change moved through. It is rare that two consecutive days record very high fire danger in Tasmania, and unprecedented in the available record that FFDI in excess of 70 should be reported on consecutive days.

b. Antecedent conditions

Precursor conditions to 12 October were themselves exceptional. Southeastern Australia was in the grip of a decade-long drought (Trewin 2006). Locally, parts of northern, central, and southeastern Tasmania experienced driest-ever winter conditions (Fig. 14). Despite some reasonable rainfall during September, record-low year-to-date rainfalls to the end of September occurred at Hobart and a number of other locations. Finally, in the 2 weeks leading to 11 October, very high FFDI occurred on 5 days, representing a very early, severe start to the 2006–07 fire season.

c. MSLP progression

A 1038-hPa high pressure system located over the bight on 9 October (Fig. 15a) moved steadily eastward, weakening slightly to 1034 hPa, to be located over the southern New South Wales coast at 0000 UTC 10 October (Fig. 15b) as it began to direct a northwesterly airstream over Tasmania. A series of low pressure systems began to move well south of Tasmania from the evening of 10 October. At 0000 UTC on 11 October (Fig. 15c), a broad area of

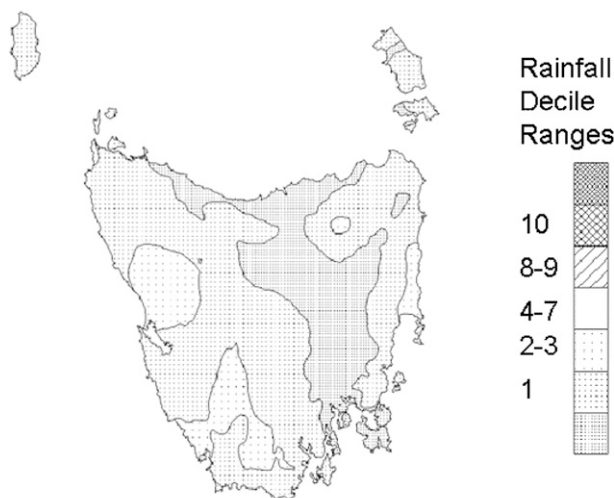


FIG. 14. Tasmanian rainfall deciles for the 3-month period 1 Jun–31 Aug 2006.

low pressure lay from about 140° to 160° E, south of 55° S, with a cold front extending from a low center within the broader trough (outside the area of the Australian region MSLP analysis) to a second low centered near 45° S, 115° E.

By 0000 UTC 12 October (Fig. 15d), the northern portion of the cold front now approaching Tasmania had

begun to weaken as most of the temperature contrast by which it had been defined became associated with a prefrontal trough that had developed from the Western Australian heat trough. At Tasmanian latitudes, however, the front maintained its structure and the pressure gradient over Tasmania tightened further as the front approached, before crossing the island in the late afternoon.

d. Upper-level analysis

A mesoLAPS 300-hPa wind speed chart is presented in Fig. 16, valid at 0300 UTC 12 October with the same boundaries as the case of 7 November 2002. A broad trough extended westward from the area of the figure, and a secondary trough was evident by slight curvature in the isotach field, particularly south of 50° S, 138° E. A broad jet extended over waters south of Australia, with embedded maxima in excess of 70 m s^{-1} , on the flanks of the secondary trough, one immediately to the southwest of Tasmania with a second south of the bight. The jet had been present in much the same location throughout the day, and persisted into the evening (not shown). Meanwhile, the embedded maxima progressed steadily eastward within the broader area of enhanced flow.

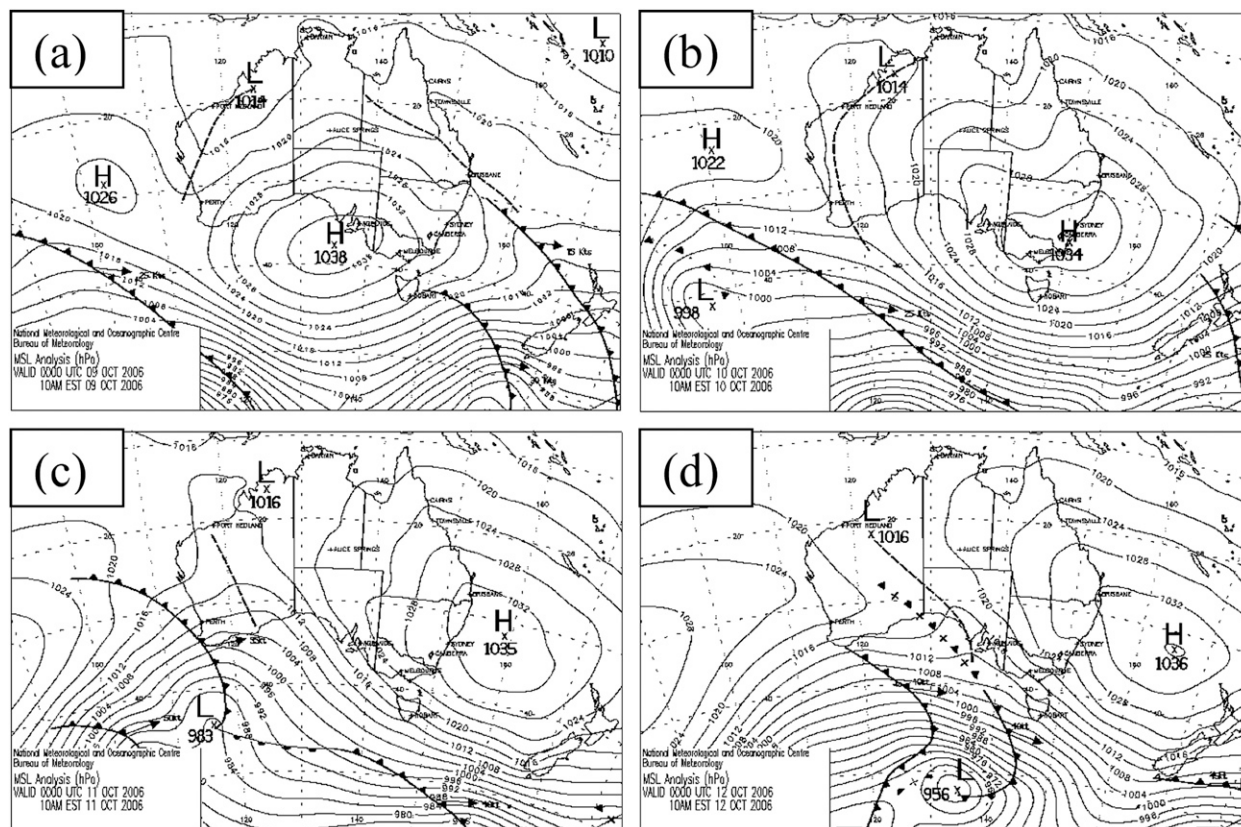


FIG. 15. MSLP analyses at 0000 UTC on (a) 9, (b) 10, (c) 11, and (d) 12 Oct 2006.

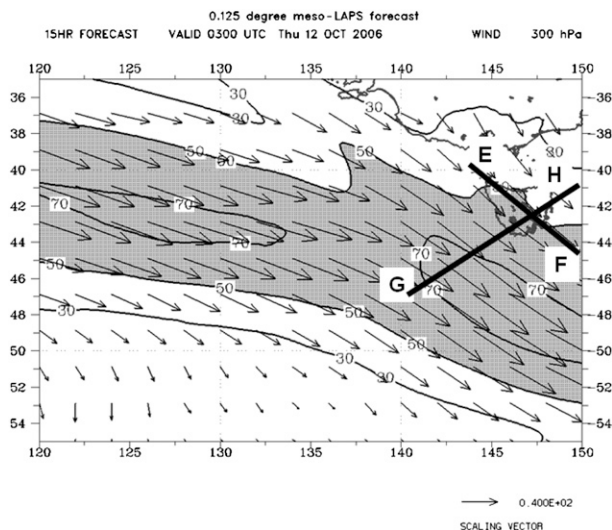


FIG. 16. MesoLAPS 300-hPa chart, as per Fig. 5, at 0300 UTC 12 Oct 2006.

e. Airmass characteristics

Low relative humidity was a particularly striking feature of early October 2006, with values below 15% (exceptional near sea level in Tasmania) on several occasions, including 11 and 12 October. At 2300 UTC 10 October (Fig. 17), a very dry layer was evident near 800 hPa. The dewpoint temperature was -35°C at that level, and was in fact negative through almost the entire troposphere. Also at around 800 hPa there was a temperature inversion of about 2°C . By 2300 UTC 11 October the air mass below 800 hPa was almost completely mixed above a very shallow radiation inversion, with the dewpoint temperature approximately -5°C through the layer. By 0100 UTC 12 October, the surface temperature at the Hobart airport was 32°C , sufficient to substantially erode the isothermal layer between about 720 and 780 hPa evident in the morning sounding, permitting dry-adiabatic mixing to at least 700 hPa, and very nearly to 600 hPa. Mixing the air mass below 700 hPa resulted in a surface dewpoint temperature around -5°C , similar to that experienced during the midmorning of 12 October (Fig. 13). For a period of several hours in the late morning and afternoon, however, the dewpoint temperature was substantially lower than that.

The source of the very dry air over Tasmania during this event was likely to have been the dry interior of continental Australia. Back trajectories from mesoLAPS were calculated as for the previous case (Fig. 18). The back trajectories indicate that the low-level (250-m elevation) air mass over Hobart at 0000 UTC 12 October had been over western Victoria some 12 or more hours earlier, and just east of Woomera around 0000 UTC 11 October,

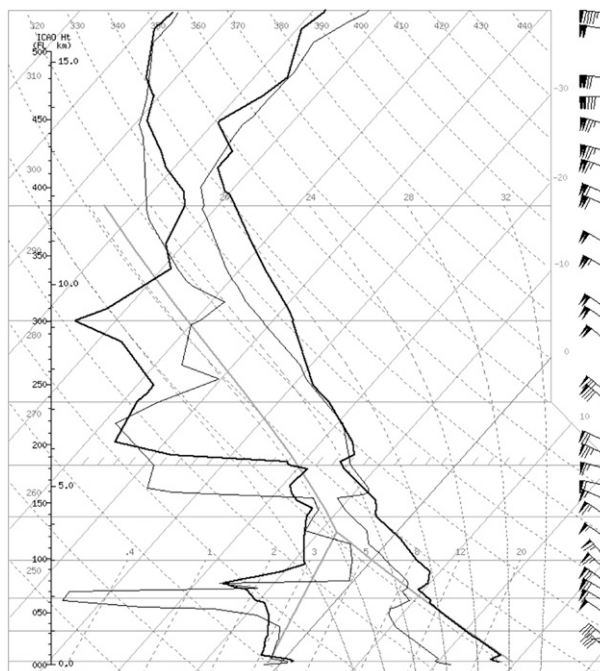


FIG. 17. Routine radiosonde flights from the Hobart airport at 2300 UTC 10 Oct (gray) and 2300 UTC 11 Oct (black).

where air parcels were modeled to have been at elevations between 500 and 1000 m. The atmospheric sounding for Woomera at 2300 UTC on 10 October (Fig. 19) is extremely dry in the lower atmosphere. The surface dewpoint was -18°C , with a resulting relative humidity below 10%. While the dewpoint temperature increased (to -9°C) immediately above the surface, it again fell abruptly near 900 hPa and was below -40°C between about 850 and 700 hPa. In the layer from which the Hobart parcels were derived, the dewpoint temperature was -10° to -11°C . Considering the moisture content of the air mass above and below this level, there was no opportunity for the admixture of more moist air into the layer. Advection of this air over Tasmania would certainly have been capable of resulting in the low relative humidity experienced during the late morning and early afternoon of 12 October, had it reached the surface.

A period of sustained descent over several days, increasing between 0000 and 1800 UTC on 10 October, is indicated by the back trajectories (Fig. 18) as air parcels followed an anticyclonically curved path. The location of the steepest descent, between about 28°S , 145°E and 32°S , 140°E , corresponds to the position of a northwest-oriented ridge extending from the high pressure center (Figs. 15b and 15c), wherein such descent might be expected, despite the generally poleward trajectory of the air parcels. This period of descent would have contributed to the warming and drying of the air mass.

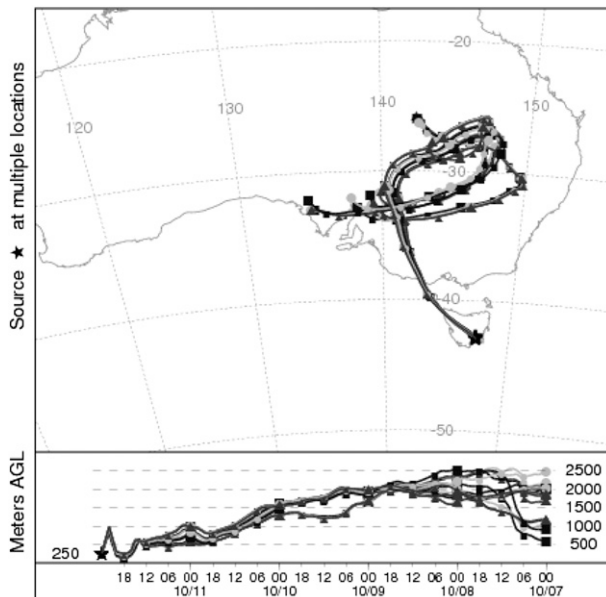


FIG. 18. Model back trajectories ending at Hobart on 0000 UTC 12 Oct 2006; details as in Fig. 9.

As the air crossed Bass Strait, there existed the possibility that it might have acquired additional moisture. Indeed, air parcels descended close to the surface near King Island while crossing Bass Strait (Fig. 18). Measurements of the air mass over Tasmania do not, however, suggest that any significant amount of moisture was entrained at that time. The arguments presented in the discussion of the airmass trajectory leading to 7 November 2002, over the Great Australian Bight, are equally valid here. Hot continental air moving over the relatively cool waters of western Bass Strait would tend to reinforce a temperature inversion atop a shallow maritime boundary layer, inhibiting mixing into the dry layer above.

f. Mesoscale features

The operational mesoLAPS model, initialized at 1200 UTC 11 October, is used for additional diagnosis of the processes resulting in the weather experienced in southeast Tasmania on 12 October. Cross sections through the path of the back trajectory between 40°S, 144°E and 45°S, 149°E (line EF in Fig. 16) reveal a pattern from early morning 12 October throughout the day consistent with a föehn wind.

Blocking of the low-level flow is evident both in observations from the north coast of Tasmania and in NWP output. Figure 20a displays the potential temperature along the cross section at 0000 UTC 12 October, with Hobart's approximate location indicated by an arrow. A well-mixed layer is evident between about 600

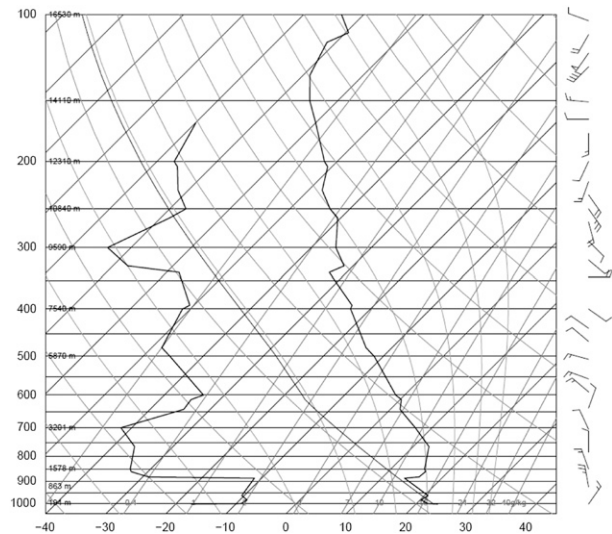


FIG. 19. Routine radiosonde trace for Woomera at 2300 UTC 10 Oct.

and 800 hPa across the breadth of the cross section, with a generally well-mixed boundary layer in the lee of the Tasmanian Central Plateau on the right side of the figure. On the northwestern (left) side of the Tasmanian orography, the potential temperature increases sharply with height, indicating a low-level maritime boundary layer, over which drier air from the Australian continent is able to flow. Observations from the north coast of Tasmania on 12 October support this conclusion. At coastal Devonport Airport the 0500 UTC temperature and dewpoint temperature were 20° and 10°C, respectively. Some 23 km inland, at 295-m elevation, Sheffield recorded temperatures of 23° and −3°C. Clearly, the maritime boundary layer was quite shallow and limited to near-coastal locations.

The forecast cross section of vertical motion, valid at 0000 UTC 12 October (Fig. 20b), is representative of the sequence of vertical motion cross sections from mesoLAPS during the day. Downward motion is indicated by solid lines, and upward vertical motion by dashed lines, scaled every 20 hPa h^{−1}. The model representation of the Tasmanian Central Plateau lies in the center of the cross section, rising to approximately 900 hPa. Strong descent is clear immediately in the lee of significant orography, with peak descent rates over the Hobart area exceeding 125 hPa h^{−1} near 850 hPa.

Visible satellite imagery from midafternoon further suggests a föehn effect (Fig. 21). Sufficient cloud is visible, which suggests the presence of a föehn wall extending from the far northwest of Tasmania over the western central plateau, with a föehn gap over southeast Tasmania. It is instructive to examine the model output

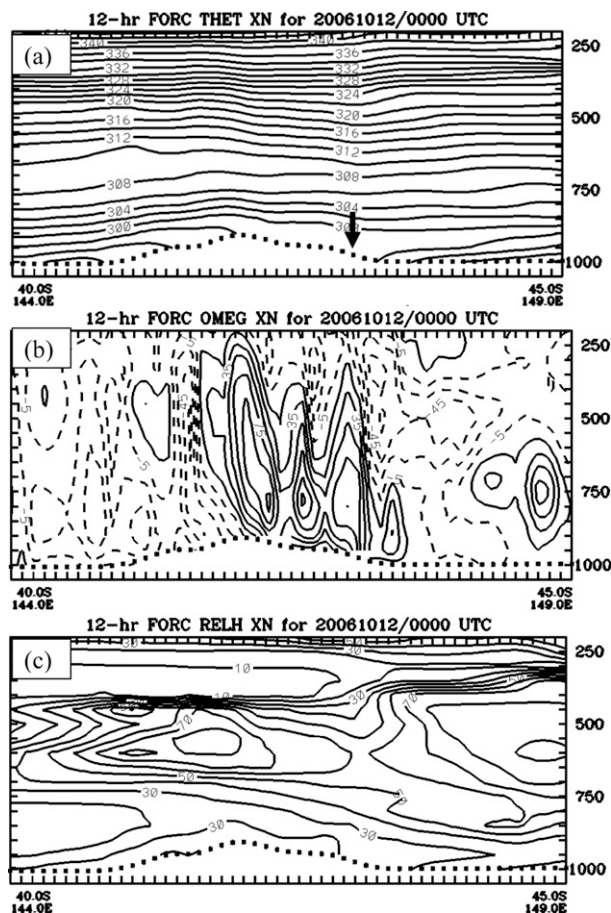


FIG. 20. Cross sections of the 12-h forecast along the line EF in Fig. 16 (40.0°S, 144.0°E to 45.0°S, 149.0°E) from the 1200 UTC 11 Oct mesoLAPS numerical model run, valid 0000 UTC 12 Oct. Approximate location of Hobart is indicated by the arrow in the top panel. Shown are (a) potential temperature isentropes (K, at intervals of 2 K), (b) vertical motion (hPa h^{-1} , with negative values dashed and contour intervals of 20 hPa h^{-1}), and (c) RH (at intervals of 10%).

relative humidity fields along the back-trajectory path above from the same model run. At the 3-h forecast time step (not shown), a layer of air with RH below 10% is evident north of the Tasmanian landmass at about 900 hPa, embedded in a broad low-level layer of dry air (RH below 30%), extending up to about 800 hPa. However, the model does not advect the driest air over the Tasmanian orography, as surface observations indicate occurs, and seems to mix out the driest layer by the 12-h forecast at 0000 UTC 12 October (Fig. 20c). It has been argued (Draper and Mills, 2008) that numerical models can have difficulty in representing accurately near-surface moisture fluxes. It seems likely in this case that the model was unable to correctly diagnose the moisture content of the air mass as it crossed the Tasmanian highlands.

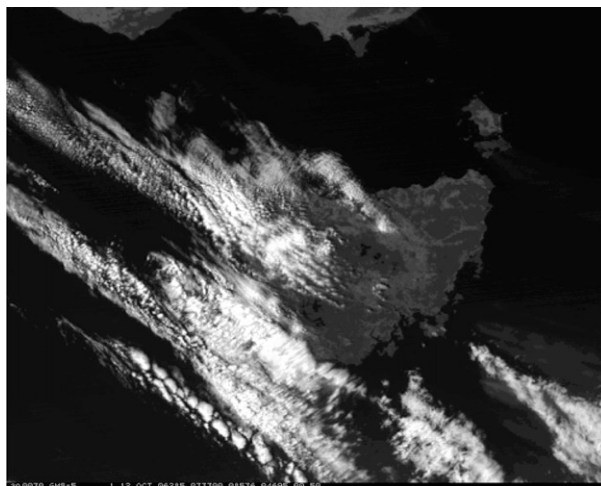


FIG. 21. Japanese Multifunctional Transport Satellite-1 (MTSAT-1) visible image of Tasmania, valid 0330 UTC 12 Oct. Frontal and prefrontal clouds are evident to the west of, and over western, Tasmania, and again to the southeast of the island. This pattern, and the absence of cloud over the southeast, is suggestive of the operation of a föehn effect at the time.

In this case, as in others cited by Sharples et al. (2010), the topographically generated downslope winds were sufficient to generate dangerous fire weather conditions. Adequate dry air preexisted within the lower troposphere, permitting the occurrence of the observed conditions, in contrast with the situation on 7 November 2002, where air was advected from higher in the atmosphere.

A 300-hPa jet streak lay to the southwest of Tasmania on 12 October 2006, in a similar location to that of 7 November 2002, yet there is no evidence from the observational record of dry-air intrusions from high in the atmosphere. Certainly, the trough axis lay considerably farther to the west during that event than during November 2002. It is, nonetheless, interesting to examine cross sections of numerical model output to ascertain details of processes operating during the day. Figure 22 represents a cross section along the line GH in Fig. 16 of the 15-h forecast mesoLAPS model atmosphere, initialized at 1200 UTC 11 October. As is the case on 7 November 2002, a tropopause depression is evident on the left of Fig. 22a, with a region of strong PVU gradient dropping from above 200 hPa to about 400 hPa, associated with the position of the jet streak (Fig. 22b). A region of anomalous PV (-0.7 PVU) extends as low as 850 hPa, with a broad area of relative humidity below 30%.

Examination of the isentropes, however, reveals an essentially horizontal orientation between approximately 700 and 850 hPa over waters west of Tasmania (left-hand side of Figs. 22a,b), such as to inhibit the transport of upper-level air any closer to the surface. This is in contrast to the situation on 7 November 2002, where isentropes

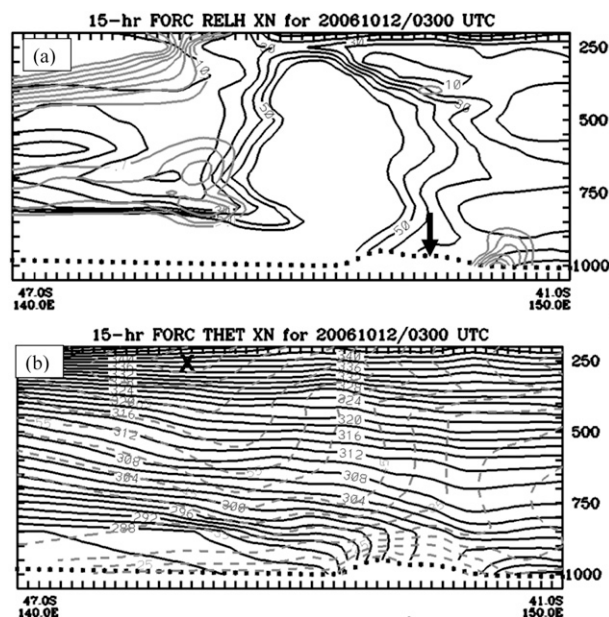


FIG. 22. MesoLAPS model cross sections through the line GH in Fig. 16 at 0300 UTC 12 Oct, showing (a) RH (black, at intervals of 10%, between 10% and 60%) and potential vorticity (gray, at intervals of 0.5 PVU between -1 and -2 PVU). The approximate location of Hobart is indicated by an arrow. (b) The potential temperature isentropes (black, at intervals of 2 K) and wind speed (gray, dashed, with isotachs at intervals of 5 m s^{-1}). The jet streak location is indicated by an \times .

slope markedly from the region of the jet streak toward the surface in the vicinity of Tasmania, enabling the progression of high-momentum, high-PV, and low-humidity air to the surface.

5. Discussion

The most dangerous fire weather experienced in Tasmania occurs with the passage of Southern Ocean cold fronts (Brotak and Reifsnnyder 1977; Marsh 1987). Springtime fire weather events follow this pattern, including the two events examined here. Further, the area experiencing heightened fire weather in each case was largely confined to eastern and particularly southeastern Tasmania, fitting the pattern of springtime fire danger discussed in Fox-Hughes (2008). In Fig. 23 are plotted peak fire dangers experienced at stations in the Tasmanian observation network on (a) 7 November 2002 and (b) 12 October 2006. Most FFDI values plotted were obtained from routine reports recorded during the events, but, as discussed above, the Hobart airport values (arrowed) were recalculated using data recorded every minute. In addition, the two bracketed values in both plots are high-level southeastern stations, both above 800 m and less representative of fire weather conditions

close to sea level. It is clear that elevated FFDI occurred predominantly in eastern and southern parts of Tasmania during both events, peaking in the southeast.

While strong winds and high temperatures contributed to the dangerous fire weather conditions observed, both of these springtime fire weather events were characterized particularly by extremely low dewpoint temperatures. The recording of a -14°C dewpoint temperature at the Hobart airport on 12 October 2006 is lower than that on all but two other days (the latter including 11 October 2006). In a database of airport weather reports between 1990 and 2008, the observation ranks equal to the fifth lowest of the 322 000 observations. The lowest dewpoint temperature recorded on 7 November 2002 puts it at seventh in the same ranking scale, with only 16 observations of the same dataset recording a lower dewpoint temperature. It is noteworthy that of the 7 days recording such low dewpoints, 6 fall within the spring months of September–November, with 5 in October–November.

The documentation of each case study above indicates that there were a number of similarities in the mechanisms acting to cause surface drying. In both events studied, air was advected over Tasmania from the Australian continental interior ahead of approaching cold fronts, and slowly descended around the flanks of high pressure systems (Figs. 4 and 9 in the case of 7 November 2002, and Figs. 15 and 18 in the case of 12 October 2006). At these times, the regions from which air was advected over Tasmania were drought affected and the air columns were consequently very dry (Figs. 8b and 19). Notably, the trajectories in each case originate over substantially different parts of continental Australia.

In both events, a föehn effect was evident and associated mountain wave activity, together with thermal mixing, acted to bring the advected dry air to the surface (Figs. 12a,b and Figs. 20a,b). This aspect of both cases is not uncommon in other documented fire weather events. Sharples et al. (2010) note the association between föehn winds and fire weather documented in a number of locations around the world, and document occurrences in southeastern Australia. Moritz et al. (2010) in particular point to the correlation between the preferred locations of modeled föehnlike Santa Ana winds of southern California and historical patterns of large wildfire activity. Mills (2008) discusses the requirement for atmospheric processes to act in concert to produce surface drying: one process to supply dry air to mid- or low levels and a further process such as thermal or turbulent mixing over topography to occur to bring the dry air to the surface.

The coupling of such processes is suggested in Fig. 24, a scatterplot of 850-hPa dewpoint depression (difference between dry-bulb and dewpoint temperatures) against wind speed at the same level, from routine morning

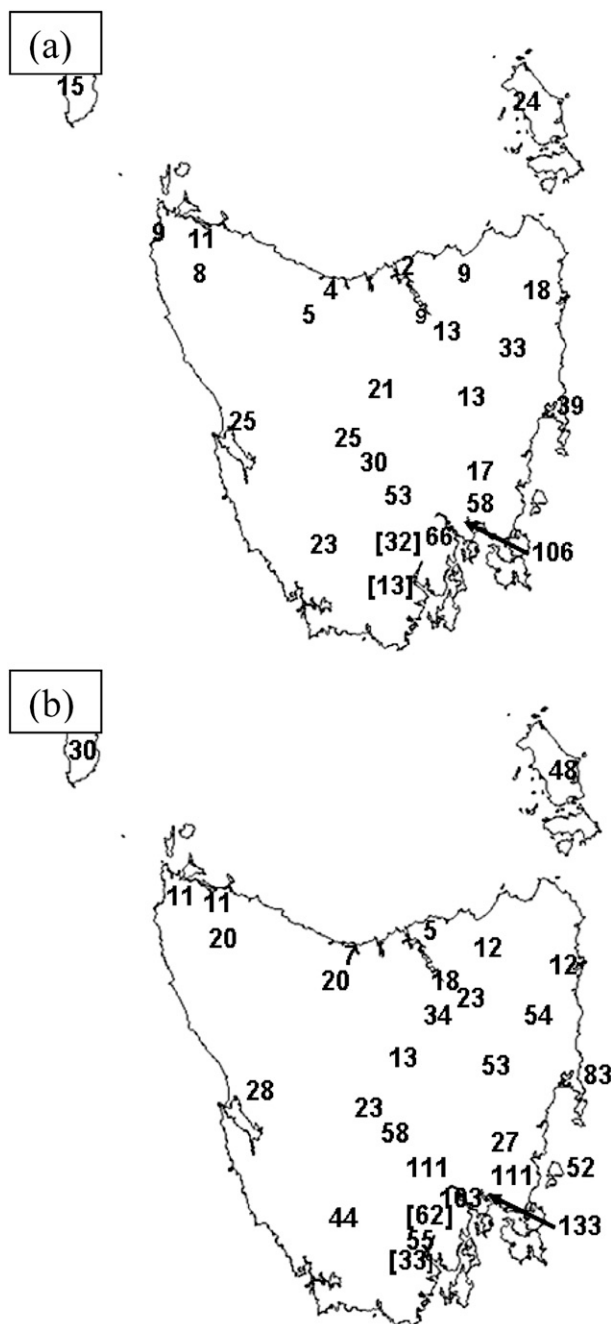


FIG. 23. Peak McArthur FFDI values recorded on (a) 7 Nov 2002 and (b) 12 Oct 2006. In both diagrams, Hobart airport values were computed from the 1-min data stream, as discussed in the text. Values for other locations were obtained from routine AWS reports during the day.

radiosonde flights at the Hobart airport between 1992 and 2010. Here, it is assumed that higher wind speed at mountaintop height is likely to result in the generation of mountain waves, with some degree of efficiency, resulting in dry air aloft mixing to the surface. Data points

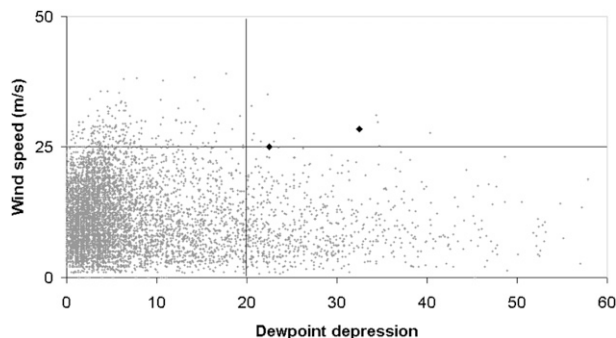


FIG. 24. Scatterplot of Hobart airport 850-hPa wind speed (m s^{-1}) and dewpoint depression ($^{\circ}\text{C}$) from routine 2200 or 2300 UTC (0900 local time) radiosonde soundings between 1992 and 2010. The two case study values are indicated by black diamonds. Threshold values of 25 m s^{-1} and 20°C , as discussed in the text, are represented by gridlines.

corresponding to the two case studies are represented by black diamonds. On 7 November 2002, the wind speed was 28.4 m s^{-1} with a dewpoint depression of 32.5°C , while on 12 October 2003 corresponding values were 25 m s^{-1} and 22.5°C . The two cases lie at the upper-right extreme of the plot. Most points lie in the lower-left corner of the plot, corresponding to relatively light winds and small dewpoint depression. Some cases exhibit very large dewpoint depression ($>50^{\circ}\text{C}$), but these generally are associated with light winds and are, hence, likely to result from the presence of subsidence inversions associated with high pressure systems. It should be noted that extreme nonlinearity of the dewpoint calculation at such low humidities makes exact values uncertain; however, it remains the case that the air mass is exceptionally dry on such occasions. MSLP analyses of the relatively few days corresponding to these parameter values confirm that they are largely days on which high pressure systems or ridges are close to Tasmania. Partitioning the plot at 25 m s^{-1} and 20°C results in only 12 data points in the upper-right quadrant. Of those during the October–March fire season (eight cases), five were days of significant fire danger while the others were affected by prefrontal cloud. This analysis, abstracting common features of the spring-time cases examined, may help alert forecasters to potential fire weather events some days ahead and provide a useful flag for fire weather events in climate change studies with large-scale general circulation models.

In addition to the mechanism outlined above, it is very likely that additional processes operated on 7 November 2002. A pulse of exceptionally dry air is evident in the plot of weather data from the Hobart airport automatic weather station (AWS; Fig. 2) in the late afternoon, some hours after thermal mixing occurred to bring preexisting dry air to the surface. There is good evidence from numerical weather guidance (Fig. 10a) that an intrusion of

stratospheric air occurred to below 900 hPa with the approach of a trough and associated cold front. The band of drier air associated with the intrusion can be seen in satellite imagery close to the time indicated in the numerical guidance (Fig. 7). With thermal and/or turbulent mixing occurring to at least 3000 m (Fig. 10b), the intrusion's dry, high-momentum air then mixed to the surface, resulting in the observed spike in weather parameters.

Investigation of these cases studies suggests techniques for forecasters to evaluate future events. Operational numerical weather prediction models are clearly capable of resolving the origins of environmental dry air in many cases. Visualizations, including vertical cross sections, of model output displaying such fields as PV, relative humidity, and potential temperature may offer valuable clues to the likelihood of occurrence of rapidly escalating fire danger ahead of cold fronts. The 2002 case demonstrates that an awareness of a stratospheric intrusion can be important for fire weather forecasters and managers. Even after the atmosphere has become fully mixed during an already dangerous fire weather event, the movement into an area of such an intrusion can result in a substantial increase in observed fire danger levels. The analysis also confirms the value of water vapor imagery as an indicator of potential dry air descent in such situations.

In the future, a synoptic climatology of Tasmanian springtime fire weather events will be undertaken, placing the occurrences of dangerous springtime events into broader context, to further improve our understanding of these weather systems. This will result in improved forecasts of dangerous fire weather, and better outcomes for the community.

Acknowledgments. Several colleagues at the Australian Bureau of Meteorology assisted in the preparation of this paper. Graham Mills reviewed drafts and offered helpful suggestions, Alan Wain facilitated back-trajectory figures, Lawrie Rikus prepared pseudo-WV imagery, and Bert Berzins extracted archived satellite imagery. Kelvin Michael of the University of Tasmania's Institute for Marine and Antarctic Studies reviewed a draft of this paper. Figure 1 was prepared using the Jules map server (www.unavco.org), and the atmospheric soundings in Figures 8a, 8b, and 19 were generated from the University of Wyoming Department of Atmospheric Science server.

REFERENCES

- Bond, H. G., K. MacKinnon, and P. F. Noar, 1967: Report on the meteorological aspects of the catastrophic bushfires in south-eastern Tasmania on 7 February 1967. Bureau of Meteorology Rep., 17 pp.
- Brotak, E. A., and W. E. Reifsnyder, 1977: An investigation of the synoptic situations associated with major wildland fires. *J. Appl. Meteor.*, **16**, 867–870.
- Bureau of Meteorology, 1985: Report on the meteorological aspects of the Ash Wednesday fires—16 February 1983. Bureau of Meteorology Rep., 143 pp.
- , 2002: Monthly weather review Tasmania for November 2002. Bureau of Meteorology Rep., 23 pp.
- , 2003: Meteorological aspects of the eastern Victorian fires January–March 2003. Bureau of Meteorology Rep., 82 pp.
- Charney, J. J., and D. Keyser, 2010: Mesoscale model simulation of the meteorological conditions during the 2 June 2002 Double Trouble State Park wildfire. *Int. J. Wildland Fire*, **19**, 427–448.
- Draper, C., and G. Mills, 2008: The atmospheric water balance over the semi arid Murray–Darling basin. *J. Hydrometeorol.*, **9**, 521–534.
- Draxler, R. R., and G. D. Hess, 1998: An overview of the HYSPLIT_4 modelling system for trajectories, dispersion, and deposition. *Aust. Meteor. Mag.*, **47**, 295–308.
- Fox-Hughes, P., 2008: A fire danger climatology for Tasmania. *Aust. Meteor. Mag.*, **57**, 109–120.
- Georgiev, C. G., and F. Martin, 2001: Use of potential vorticity fields, Meteosat water vapour imagery and pseudo water vapour images for evaluating numerical model behaviour. *Meteor. Appl.*, **8**, 57–69.
- Hanstrum, B. N., K. J. Wilson, and S. L. Barrell, 1990: Prefrontal troughs over southern Australia. Part I: A climatology. *Wea. Forecasting*, **5**, 22–31.
- Huang, C., Y.-L. Lin, M. L. Kaplan, and J. J. Charney, 2009: Synoptic-scale and mesoscale environments conducive to forest fires during the October 2003 extreme fire event in Southern California. *J. Appl. Meteor. Climatol.*, **48**, 553–579.
- Luke, R. H., and A. G. McArthur, 1978: *Bushfires in Australia*. Australian Government Publishing Service, 359 pp.
- Marsh, L., 1987: Fire weather forecasting in Tasmania. Meteorological Note 171, Bureau of Meteorology, 47 pp.
- McArthur, A. G., 1967: Fire behaviour in eucalypt forests. Forestry and Timber Bureau Leaflet 107, Australian Government, 25 pp.
- McLeod, R. N., 2003: Inquiry into the operational response to the January 2003 bushfires in the ACT. Publ. 03/0537, Dept. of Urban Services, 273 pp.
- Mills, G., 2005a: A re-examination of the synoptic and mesoscale meteorology of Ash Wednesday 1983. *Aust. Meteor. Mag.*, **54**, 35–55.
- , 2005b: On the subsynoptic-scale meteorology of two extreme fire weather days during the eastern Australian fires of January 2003. *Aust. Meteor. Mag.*, **54**, 265–290.
- , 2008: Abrupt surface drying and fire weather. Part 2: A preliminary synoptic climatology in the forested areas of southern Australia. *Aust. Meteor. Mag.*, **57**, 311–328.
- Moritz, M. A., T. J. Moody, M. A. Krawchuk, M. Hughes, and A. Hall, 2010: Spatial variation in extreme winds predicts large wildfire locations. *Geophys. Res. Lett.*, **37**, L04801, doi:10.1029/2009GL041735.
- Nairn, J., J. Prideaux, D. Ray, D. Tippins, and A. Watson, 2005: Meteorological report on the Wangary and Black Tuesday fires, Lower Eyre Peninsula, 10–11 January 2005. Bureau of Meteorology Rep., 64 pp.
- Puri, K., G. D. Dietachmayer, G. A. Mills, N. E. Davidson, R. A. Bowen, and L. W. Logan, 1998: The new BMRC Limited Area Prediction System, LAPS. *Aust. Meteor. Mag.*, **47**, 203–223.

- Sharples, J. J., G. A. Mills, R. H. D. McRae, and R. O. Weber, 2010: Foehn-like winds and elevated fire danger in southeastern Australia. *J. Appl. Meteor. Climatol.*, **49**, 1067–1095.
- Stocks, B. J., and T. J. Lynham, 1996: Fire weather climatology in Canada and Russia. *Fire in Ecosystems of Boreal Eurasia*, J. G. Goldammer and V. V. Furyaev, Eds., Kluwer Academic, 481–487.
- Taylor, J., and R. M. Webb, 2004: Meteorological aspects of the 2002/2003 bushfire season in NSW. *Proc. 11th Annual AFAC Conf. and Inaugural Bushfire CRC Conf.*, Perth, WA, Australia, Australasian Fire and Emergency Service Authorities Council, 349–358.
- Trewin, B. C., 2006: An exceptionally dry decade in parts of southern and eastern Australia October 1996–September 2006. Special Climate Statement 9, Australian National Climate Center, 9 pp.
- Valendik, E. N., G. A. Ivanova, Z. O. Chuluunbator, and J. G. Goldammer, 1998: Fire in forest ecosystems of Mongolia. *Int. For. Fire News*, **19**, 58–63.
- Westerling, A. L., H. G. Hidalgo, D. R. Cayan, and T. W. Swetnam, 2006: Warming and earlier spring increase western U.S. forest wildfire activity. *Science*, **313**, 940–943.
- Zimet, T., J. E. Martin, and B. E. Potter, 2007: The influence of an upper-level frontal zone on the Mack Lake wildfire environment. *Meteor. Appl.*, **14**, 131–147.